GEOPHYSICAL RESEARCH LETTERS, VOL. 27, NO. 13, PAGES 1871-1874, JULY 1, 2000

Oxygen Auger electrons observed in Mars' ionosphere

D. L. Mitchell[1], R. P. Lin[1,2], H. Rème[3], D. H. Crider[4], P. A. Cloutier[5], J. E. P. Connerney[6], M. H. Acuña[6], and N. F. Ness[7]

Abstract. Over the course of 290 orbits, the Electron Reflectometer onboard Mars Global Surveyor consistently observed a plasma boundary at a median altitude of 380 km, where electron fluxes at energies greater than ∼100 eV change abruptly by about an order of magnitude. Above the boundary, electron energy spectra are consistent with solar wind electrons that have been shocked and then cooled by impact with exospheric neutrals. Below the boundary, electron energy spectra exhibit a broad feature from 20 to 50 eV, which likely results from a blend of unresolved photoionization peaks that have been predicted by published models of ionospheric photoelectrons at Mars. We attribute a second feature at ∼500 eV to oxygen Auger electrons. The 500-eV flux level measured below the boundary responds to variations in the solar soft x-ray flux and is consistent with a balance between photoionization and loss by impact with atmospheric neutral atoms.

Introduction

After arriving at Mars on 12 September 1997 in a highly elliptical polar orbit, the Mars Global Surveyor (MGS) spacecraft aerobraked to achieve a ∼400-km-altitude circular mapping orbit. The MGS science payload includes two identical 3-axis fluxgate magnetometers (MAG) and a symmetric hemispherical electrostatic analyzer (ER), which measures the energy and angular distributions of 10 eV to 20 keV electrons [*Acuña et al.*, 1992]. Throughout most of aerobraking, periapsis was targeted for the 3.5-nanobar pressure level (∼120 km altitude), which exceeds the maximum pressure that the ER can be safely operated. (At pressures above ∼1 nanobar, there is risk of electrical discharge inside the instrument.) Because of Mars' atmospheric variability and uncertainty in predicting the time of periapsis, the ER high voltage was disabled below altitudes of ∼350 km. However, there were 390 "science phasing" orbits with periapsis at ∼170 km (0.02 nanobar), where there was ample safety margin for operating the ER. These orbits provided a unique (and unanticipated) opportunity to observe 10 eV to 20 keV electrons in Mars' ionosphere.

Previous observations of the Martian ionosphere have consisted of retarding potential analyzer (RPA) measurements during two Viking lander descents and numerous radio occultations obtained from the Mariner, Mars, and Viking orbiters. The Viking descent profiles revealed a complex topside ionosphere, but a clear Chapman layer electron density peak was observed at an altitude of ∼130 km [*Hanson et al.*, 1977]. Radio occultation observations of Mars' ionosphere have been summarized by *Hantsch and Bauer* [1990] and by *Zhang et al.* [1990a, b]. The Chapman layer peak altitude and density vary from ∼120 km and 2×10^5 cm^{-3} at the subsolar point to ∼170 km and 5×10^4 cm^{-3} near the terminator.

The radio occultation measurements are sensitive to the total electron density, which is dominated by a thermal population with a temperature ∼0.3 eV above 200 km altitude [*Hanson and Mantas*, 1988], decreasing to ∼0.02 eV near the Chapman peak [*Choi et al.*, 1998]. The Viking RPA was capable of measuring electrons with energies up to 75 eV and detected two suprathermal populations with effective temperatures of 3 eV and 17 eV [*Hanson and Mantas*, 1988]. The first was attributed to an equilibrium photoelectron gas, and the second was assumed to be solar wind leakage into the ionosphere. The ER is sensitive to the second of these suprathermal electron populations and extends the measurement energy range well beyond that of the Viking RPA.

Observations

A time series of electron and magnetic field measurements obtained on 2 April 1998 (Fig. 1) begins with the spacecraft in the magnetotail, approaching periapsis from the night hemisphere and over the north pole. The electron energy distribution in this region (Fig. 2) is similar to a solar wind distribution. Descending from 270 to 180 km altitude, the spacecraft passes through a transition region where the 840-eV flux drops by more than an order of magnitude. This is accompanied by a change in the electron energy distribution (Fig. 2), which exhibits a broad feature from 20 and 50 eV (defined by discrete changes in spectral slope), followed by sharp drop near 60 eV, and then a second feature at ∼500 eV. Outbound, the transition region is encountered from 320 to 370 km, and the spacecraft exits into the magnetosheath on the sunlit hemisphere, where the electron spectrum (Fig. 2) is consistent with a solar wind distribution that has been shocked and then cooled by impact with exospheric neutrals [*Crider et al.*, 2000].

The 10-90 eV electron population is likely the same as the higher energy suprathermal population detected by the Viking RPA. We estimate the density of 10-90 eV electrons assuming a zero spacecraft potential relative to the plasma and compare this to the Viking RPA measurements in Fig. 3. (Since MGS was in sunlight, we expect that the actual spacecraft potential was a few volts positive, which would increase our density estimate by a few tens of percent.) The MGS and Viking density estimates are similar below 300 km but diverge at higher altitudes. As we shall see, the electron density in both of these altitude ranges can vary with time

[1]Space Sciences Laboratory, Univ. of Calif., Berkeley, CA
[2]Physics Dept., Univ. of Calif., Berkeley, CA
[3]CESR, Toulouse, France
[4]NRC Fellow, NASA-GSFC, Greenbelt, MD
[5]Dept. of Physics and Astron., Rice Univ., Houston, TX
[6]NASA-GSFC, Greenbelt, MD
[7]Bartol Research Inst., Univ. of Delaware, Newark, DE

Paper number 1999GL010754.
0094-8276/00/1999GL010754$05.00

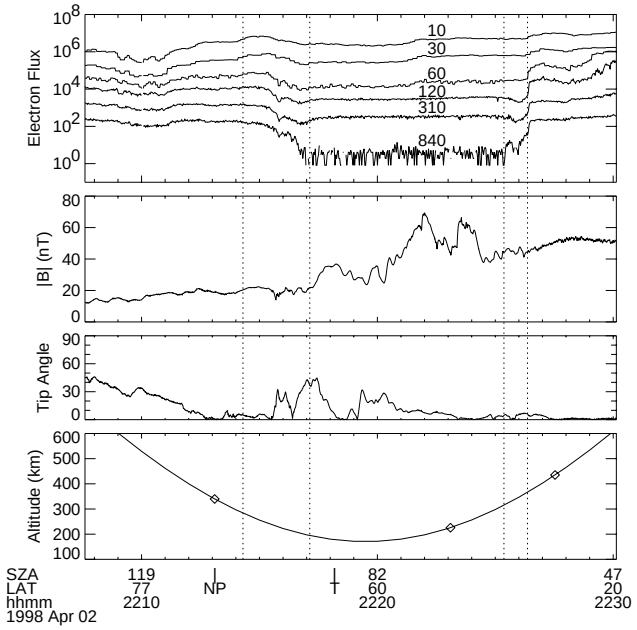

Figure 1. Time series of electron and magnetic field measurements obtained during a periapsis pass on 2 April 1998. The electron flux (cm^{-2} s^{-1} $ster^{-1}$ eV^{-1}) is averaged over the field of view in six energy channels from 10 to 840 eV. The tip angle is the angle the magnetic field vector makes with respect to the local horizontal (ranging from 0° to 90°). Symbols along the spacecraft altitude curve indicate where the electron energy spectra shown in Fig. 2 were obtained. Latitude and solar zenith angle are shown at a few points along the time axis. Times when the spacecraft passes over the north pole (NP) and crosses the terminator (T) are also indicated. Vertical dashed lines mark the inbound and outbound transition regions, which separate solar wind from ionospheric plasma.

by factors of several, depending on solar wind conditions and EUV flux, so precise agreement is not expected.

Below the transition region, the electron flux enhancement from 20-50 eV is in the same energy range as prominent photoionization peaks (Fig. 2) due to the absorption of solar line emissions by atmospheric CO_2 and O [*Fox and Dalgarno*, 1979a; *Mantas and Hanson*, 1979]. (The individual peaks would be unresolved by the ER.) The sharp flux drop measured near 60 eV is also seen in the model spectrum, corresponding to a sharp drop in the flux of ionizing radiation and a decrease in the ionization cross sections. Thus, ionospheric photoelectrons appear to dominate below the transition region, which is now seen as a boundary between solar wind plasma and planetary ionospheric plasma. The flux contrast across this boundary at energies above 60 eV (Fig. 1) implies effective magnetic separation between these two plasmas.

Since photoelectrons dominate the 10-60-eV spectrum, the feature at ∼500 eV suggests the possibility of ionization by soft x-ray photons. At the altitudes sampled by the ER, the dominant neutral gas species are expected to be H, O, and CO_2 [*Nier and McElroy*, 1976; *Fox and Dalgarno*, 1979a; *Bougher et al.*, 1990; *Kim et al.*, 1998]. When a K-shell electron is ejected from O by a soft x-ray photon (energy > 533 eV), the resulting ion relaxes by emitting photons and nearly always one or more Auger electrons, which have energies within ∼10% of 500 eV [*Moddeman et al.*, 1971]. With an energy resolution ($\Delta E/E$) of 25%, most of these excess electrons should appear in the 455-eV channel, with a small contribution to the 583-eV channel, which is consistent with the observations.

Electron fluxes at energies greater than ∼100 eV are nearly independent of altitude below the transition region, despite a steep gradient in the neutral density (Figs. 1 and 3), suggesting a steady state in which the dominant source and loss terms are proportional to the neutral density. Calculations of the steady-state photoelectron flux at Mars [*Mantas and Hanson*, 1979] show a nearly constant 40-100 eV flux above 170 km when vertical transport is prevented by a horizontal magnetic field. With an oxygen K-shell ionization cross section of $\sigma_i = 5\times10^{-19}$ cm^2, the atmosphere is optically thin ($\tau < 10^{-2}$) to soft x-rays at the altitudes and solar zenith angles sampled by the ER. Thus, a balance between photoionization and electron impact ionization, which is the dominant loss process for >100-eV electrons [*Fox and Dalgarno*, 1979b], provides an order-of-magnitude estimate of the 500-eV electron flux: $F_e \approx (1 + Y_A)\, F_x\, (\sigma_i/\sigma_{ei})$, where Y_A is the Auger yield, $F_x \approx 4\times10^7$ photons cm^{-2} s^{-1} is the soft x-ray flux ($\lambda < 2.3$ nm) [*Tobiska and Eparvier*, 1997], and $\sigma_{ei} \approx 10^{-16}$ cm^2 is the electron impact ionization cross section [*Orient and Srivastava*, 1987; *Itakawa and Ichimura*, 1990]. If these electrons are isotropic and have energies within 10% of 500 eV, then the predicted differential

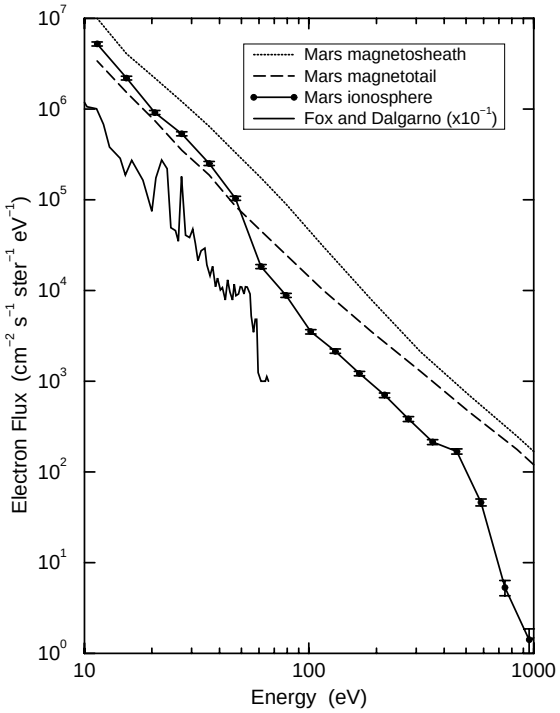

Figure 2. Electron flux vs. energy at different locations along the orbit shown in Fig. 1: the magnetotail at 340 km altitude inbound; the ionosphere at 225 km outbound, and the magnetosheath at 435 km outbound. The ER energy channels are indicated by the filled circles with error bars on the ionospheric spectrum. Error bars account for only counting statistics and digitization noise. We assume that the magnetic field and plasma are stationary during the 12-sec accumulation time for each spectrum. A model photoelectron spectrum for the Martian ionosphere at an altitude of 130 km [*Fox et al.,* 1979a] is offset below the observed spectra.

electron flux would be ∼160 cm^{-2} s^{-1} ster^{-1} eV^{-1}, which is comparable to the measured value.

The next most abundant element is carbon, with roughly 10% of the concentration of oxygen atoms at 225 km. Carbon contributes Auger electrons at ∼250 eV; however, no feature is observed near this energy. A calculation similar to the one above yields an expected differential electron flux of ∼270 cm^{-2} s^{-1} ster^{-1} eV^{-1} at 250 eV, which is half of the measured value. Evidently, the carbon Auger peak is too weak to be detected, perhaps partly because it falls midway between two ER energy channels.

Soft X-ray control of Auger electrons

The production of Auger electrons should respond to changes in the solar soft x-ray flux ($\lambda < 2.3$ nm), which is strongly modulated by active regions and flares. Active regions evolve on time scales of days to weeks, and flares typically last for minutes. Since any particular active region may not be visible simultaneously from Earth and Mars, we must take into account solar rotation when comparing x-ray measurements at Earth with electron measurements at Mars. The solar rotation period is ∼25 days at the equator, increasing to ∼28 days at 40° latitude. Thus, it can take up to two weeks for an active region to rotate from facing Earth to facing Mars, during which time that region's x-ray production can change significantly. The solar x-ray energy flux at a wavelength of ∼1 nm, as measured by YOHKOH with the AlMg filter, is shown in Fig. 4. Each x-ray data point is shifted on the time axis by the amount of time it takes a point on the sun to rotate from the sub-Earth to the sub-Mars longitude, assuming a 26-day rotation period. The x-ray data are then median averaged at the 12-hour orbital period of MGS. This filters out solar flares, but since the MGS observations were obtained near conjunction, it is unlikely for a flare to be seen simultaneously from Earth and Mars.

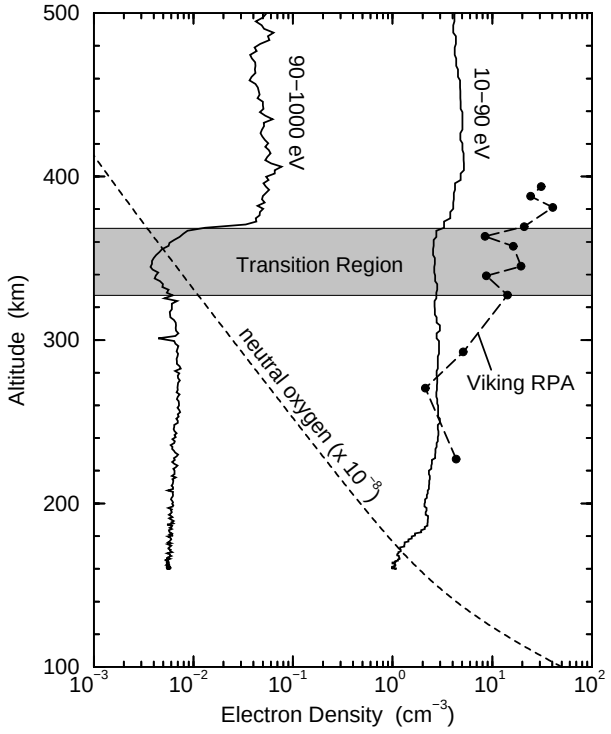

Figure 3. Vertical profiles of the electron density in two energy ranges obtained outbound from periapsis on the orbit shown in Fig. 1. The density profile of a suprathermal electron population (T = 17 eV) measured by the Viking 1 RPA [*Hanson and Mantas,* 1988] is shown for comparison. The neutral oxygen density is from *Kim et al.* [1998].

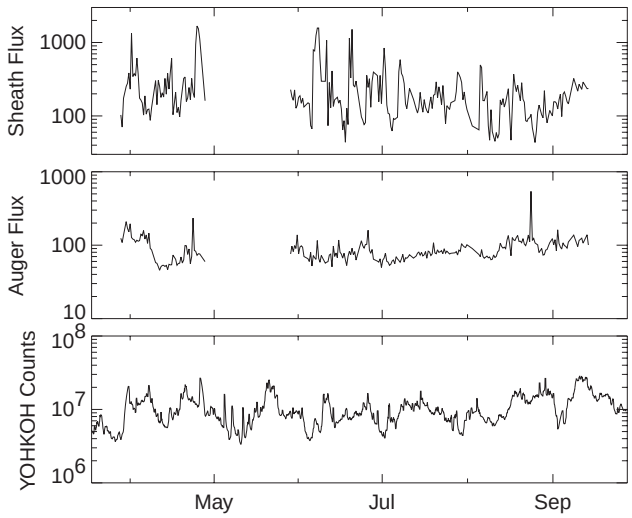

Figure 4. The 500-eV electron flux measured in the magnetosheath and in the ionosphere during each periapsis pass from 28 March to 13 September 1988. The x-ray energy flux measured by the YOHKOH satellite in Earth orbit has been shifted along the time axis to account for the different orbital positions of Earth and Mars (see text). A gap in the measurements (4/28 - 5/27) occurs around conjunction, when the Sun blocked communications with the spacecraft.

The 500-eV electron flux measured within the ionosphere during each periapsis pass is shown for comparison with the time-shifted x-ray data. A rank correlation test indicates a positive correlation ($\rho = 0.4$) with a negligible probability ($< 10^{-8}$) of occurring by chance when the assumed solar rotation period is between 25 and 28 days. The correlation rapidly degrades for rotation periods less than 20 days or greater then 30 days. Visually, the correlation appears excellent during April 1998 but marginal from June to September 1998, which could result from the evolution of active regions. On August 24 (orbit 510), the 500-eV photoelectron flux was a factor of five larger than measured on adjacent orbits, probably in response to a solar flare. A similar flare response was observed on April 23 (orbit 257). The 500-eV magnetosheath electron flux measured just above the plasma boundary is also shown for comparison with the ionospheric flux (Fig. 4). The sheath flux is uncorrelated with the Auger and x-ray fluxes.

These observations reveal the existence of a persistent plasma boundary that separates Mars' ionosphere from the solar wind. Over the course of 290 orbits, the median altitude of the boundary on the sunlit hemisphere was 380 km, with most crossings between 200 and 800 km.

Acknowledgments. The research was supported at Berkeley by NASA grant NAG-5-959 and at Rice under NASA grant NGT-5-34. We thank Brian Flynn for help in processing the solar F10.7 data and James McTiernan for assistance with the YOHKOH data.

References

Acuña, M. H., J. E. P. Connerney, P. Wasilewski, R. P. Lin, K. A. Anderson, C. W. Carlson, J. McFadden, D. W. Curtis, H. Rème, A. Cros, J. L. Medale, J. A. Sauvaud, C. d'Uston, S. J. Bauer, P. Cloutier, M. Mayhew, and N. F. Ness, Mars Observer magnetic fields investigation, *J. Geophys. Res., 97,* 7799, 1992.

Bougher, S. W., R. G. Roble, E. C. Ridley, and R. E. Dickinson, The Mars thermosphere, 2, General circulation with coupled dynamics and composition, *J. Geophys. Res., 95,* 14811, 1990.

Choi, Y. W., J. Kim, K. W. Min, A. F. Nagy, and K. I. Oyama, Effect of the magnetic field on the energetics of Mars ionosphere, *Geophys. Res. Lett., 25,* 2753, 1998.

Crider, D. H., P. A. Cloutier, C. C. Law, P. W. Walker, Y. Chen, M. H. Acuña, J. E. P. Connerney, D. L. Mitchell, R. P. Lin, K. A. Anderson, C. W. Carlson, J. P. McFadden, H. Rème, C. Mazelle, C. d'Uston, J. A. Sauvaud, D. Vignes, D. A. Brain, and N. F. Ness, Evidence for electron impact ionization in the magnetic pileup boundary of Mars, *Geophys. Res. Lett., 27,* 45, 2000.

Fox, J. L., and A. Dalgarno, Ionization, luminosity, and heating of the upper atmosphere of Mars, *J. Geophys. Res., 84,* 7315, 1979.

Fox, J. L., and A. Dalgarno, Electron energy deposition in carbon dioxide, *Planet. Space Sci., 27,* 491, 1979.

Hanson, W. B., S. Sanatani, and D. R. Zuccaro, The martian ionosphere as observed by the Viking retarding potential analyzer, *J. Geophys. Res., 82,* 4351, 1977.

Hanson, W. B., and G. P. Mantas, Viking electron temperature measurements: Evidence for a magnetic field in the Martian ionosphere, *J. Geophys. Res., 93,* 7538, 1988.

Hantsch, M. H., and S. J. Bauer, Solar control of the Mars ionosphere, *Planet. Space Sci., 38,* 539, 1990.

Itakawa, Y., and A. Ichimura, Cross sections for collisions of electrons and photons with atomic oxygen, *J. Phys. Chem. Ref. Data, 19,* 637, 1990.

Kim, J., A. F. Nagy, J. L. Fox, and T. E. Cravens, Solar cycle variability of hot oxygen atoms at Mars, *J. Geophys. Res., 103,* 29339, 1998.

Mantas, G. P., and W. B. Hanson, Photoelectron fluxes in the Martian ionosphere, *J. Geophys. Res., 84,* 369, 1979.

Moddeman, W. E., T. A. Carlson, M. O. Krause, B. P. Pullen, W. E. Bull, and G. K. Schweitzer, Determination of the K-LL Auger spectra of N_2, O_2, CO, NO, H_2O, and CO_2, *J. Chem. Phys., 55,* 2317, 1971.

Nier, A. O., and M. B. McElroy, Structure of the neutral upper atmosphere of Mars: Results from Viking 1 and Viking 2, *Science, 194,* 1298, 1976.

Orient, O. J., and S. K. Srivastava, Electron impact ionisation of H_2O, CO, CO_2, and CH_4, *J. Phys. B: At. Mol. Phys., 20,* 3923, 1987.

Tobiska, W. K., and F. E. Eparvier, EUV97: Improvements to EUV irradiance modeling in the soft x-rays and FUV, *Solar Physics, 177,* 147, 1997.

Zhang, M. H. G., J. G. Luhmann, A. J. Kliore, and J. Kim, A post-Pioneer Venus reassessment of the Martian dayside ionosphere as observed by radio occultation methods, *J. Geophys. Res., 95,* 14829, 1990a.

Zhang, M. H. G., J. G. Luhmann, A. J. Kliore, An observational study of the nightside ionospheres of Mars and Venus with radio occultation methods, *J. Geophys. Res., 95,* 17095, 1990b.

R. P. Lin and D. L. Mitchell, Space Sciences Laboratory University of California Berkeley, CA 94720. (e-mail:mitchell@ssl.berkeley.edu)

H. Rème, Centre d'Etude Spatiale des Rayonnements, 31028 Toulouse Cedex 4, France.

D. H. Crider, NRC Fellow, NASA Goddard Space Flight Center, Greenbelt, MD 20771.

P. A. Cloutier, Department of Physics and Astronomy, Rice University, Houston, TX 77005.

M. H. Acuña and, J. E. P. Connerney NASA Goddard Space Flight Center, Greenbelt, MD 20771.

N. F. Ness, Bartol Research Institute, University of Delaware, Newark, DE 19716.

(Received October 27, 1999; revised January 28, 2000; accepted March 13, 2000.)